



Dose to contralateral breast from whole breast irradiation by automated tangential IMRT planning: comparison of flattening-filter and flattening-filter-free modes

Ichiro Ogino¹, Hidetaka Seto^{1,2}, Daisuke Shigenaga¹, Masaharu Hata³

¹Department of Radiation Oncology, Yokohama City University Medical Center, Yokohama, Japan

²Department of Radiation Oncology, Ishikawa Prefectural Central Hospital, Ishikawa, Japan

³Division of Radiation Oncology, Department of Oncology, Yokohama City University Graduate School of Medicine, Yokohama, Japan

ABSTRACT

Background: The most common secondary cancer is contralateral breast (CLB) cancer after whole breast irradiation (WBI). The aim of this study was to quantify the reduction of CLB dose in tangential intensity modulated radiotherapy (t-IMRT) for WBI using flattening-filter-free (FFF) beams.

Materials and methods: We generated automated planning of 20 young breast cancer patients with limited user interaction. Dose-volume histograms of the planning target volume (PTV), ipsilateral lung, heart, and CLB were calculated. The dose of PTV, the most medial CLB point, and the CLB point below the nipple was measured using an ionization chamber inserted in a slab phantom. We compared the two t-IMRT plans generated by FFF beams and flattening-filter (FF) beams.

Results: All plans were clinically acceptable. There was no difference in the conformal index, the homogeneity for FFF was significantly worse. For the ipsilateral lung, the maximum dose (D_{max}) was significantly higher; however, V_{20} showed a tendency to be lower in the FFF plan. No differences were found in the D_{max} and V_{30} to the heart of the left breast cancer. FF planning showed significantly lower D_{max} and mean dose to the CLB. In contrast to the calculation results, the measured dose of the most medial CLB point and the CLB point below the nipple were significantly lower in FFF mode than in FF mode, with mean reductions of 21.1% and 20%, respectively.

Conclusions: T-IMRT planning using FFF reduced the measured out-of-field dose of the most medial CLB point and the CLB point below the nipple.

Key words: young breast cancer; contralateral breast; whole breast irradiation; tangential intensity modulated radiotherapy; flattening-filter-free

Rep Pract Oncol Radiother 2022;27(1):113-120

Introduction

Whole breast irradiation (WBI) after breast-conserving surgery is the standard treatment for early-stage breast cancer. In patients treated with WBI, the most common secondary cancer is contralateral

breast (CLB) cancer. Several studies found the risk of CLB cancer to be evident among young women (age < 45 years) treated with radiotherapy and followed for ≥ 5 years [1, 2]. Stovall et al. [3] found that a significantly higher proportion of CLB cancers were located in the inner and central quadrants

Address for correspondence: Ichiro Ogino MD, Department of Radiation Oncology, Yokohama City University Medical Center, 4-57 Urafune-cho, Minami-ku, Yokohama, Kanagawa, 232-0024, Japan; e-mail: ogino1ro@yokohama-cu.jp

This article is available in open access under Creative Commons Attribution-Non-Commercial-No Derivatives 4.0 International (CC BY-NC-ND 4.0) license, allowing to download articles and share them with others as long as they credit the authors and the publisher, but without permission to change them in any way or use them commercially

for irradiated women. Women aged < 40 years with higher CLB radiation dose exposure had a threefold greater risk than no or lower-dose-exposed women at follow-up periods > 5 years.

An out-of-field dose to the CLB is not desirable in WBI. The out-of-field dose consists of three main components: head leakage, internal scatter, and collimator scatter [4]. While head leakage is reduced by flattening-filter-free (FFF) beams [4, 5], studies reporting the CLB dose of FFF beams in WBI are limited [6].

Most reports regarding CLB cancer risk were conducted using commercial treatment planning systems (TPS) [7, 8]. However, commercial TPS are not recommended for accurate out-of-field dose assessment [9]. Previous studies used CLB doses measured in a phantom to estimate the risk of subsequent breast cancer. This method involves the dose corresponding to head leakage [10, 12].

The aim of this study was to quantify the reduction of CLB dose from tangential intensity modulated radiotherapy (t-IMRT) for WBI using FFF beams. We generated an automated planning process with limited user interaction, and compared the results with those of flattening-filter (FF) beams by means of TPS calculations and Farmer ionization chamber (IC) measurements.

Materials and methods

Patients and treatment planning

Planning computed tomography (CT) datasets of ten right and ten left breast cancer female patients were used for this study. All patients were aged < 40 years (range, 28–39 years) and had WBI after breast-conserving surgery between 2013 and 2019. These 20 patients were retrospectively re-planned with limited user interaction in the treatment planning process. The institutional review board (approval number: B180500020) approved the study protocol, which was carried out in accordance with the declaration of Helsinki of 1975 (as revised in 2008).

The CT datasets were acquired on a four-slice CT scanner (Lightspeed; GE Medical System, Waukesha, WI, USA) with a 2.5-mm slice thickness. Radio-opaque wire was placed around the palpable breast tissue at the time of CT simulation to identify the superior, inferior, medial and lateral markers that covered the peripheral breast tissue. Treatment

planning was conducted using the Pinnacle³ TPS (v. 9.14; Philips Radiation Oncology Systems, Fitchburg, WI). Dose calculations of the treatment plans were performed using the superposition algorithm with a grid resolution of 3 mm.

The treatment planning process was based on a previous report, and mostly followed the guidelines [13]. Medial and lateral tangential treatment beams with half-beam block were created. A medial marker was positioned 1.0 cm medial to the radio-opaque wire. Lateral, superior, and inferior markers were located 1.5 cm posterolateral, superior, and inferior to the wire, respectively. The superior and inferior edges of the tangent beams intersected the superior and inferior markers with the cranio-caudally symmetric beam. The posterior edges of the tangent beams intersected the medial and lateral markers. The anterior borders with skin flash were 2 cm from the nipple. The beam isocenter was located at the midpoint of the medial and lateral markers (Fig. 1A). User interaction was limited to these anatomic landmarks identified on CT simulation and the collimator angle which were set as the posterior edge of the beam parallel to the chest wall.

Delineation of the lungs and heart was performed automatically using the Pinnacle³ Auto-Segmentation function. The CLB was delineated by a single radiation oncologist (DS) using the atlas proposed by the Radiation Therapy Oncology Group [14]. To define the treatment volume of ipsilateral breast, the 55% isodose level irradiated by the tangent beams was initially contoured. After excluding organs at risk (OAR) from the 55% isodose level contour, the planning target volume (PTV) for optimization was generated with the volume contracted by 5 mm in the axial plane and 10 mm in the cranio-caudal direction [13].

For each of the 20 patients, treatment plans were created with both conventional FF and FFF 6-MV photon beams of TrueBeam (Varian Medical Systems, Palo Alto, CA, USA). FFF beams provide higher dose rates (1400 monitor units [MU]/min) than FF beams (600 MU/min). With a prescription of 200 cGy per fraction for a total of 25 fractions, 80% of the dose was delivered by the opposed open beams calculated at the breast point (Fig. 1A), and 20% was delivered by two opposed step-and-shoot IMRT beams with gantry angle, collimator angle, and beam isocenter constant. Optimization parameters, the minimum segment area, and maximum

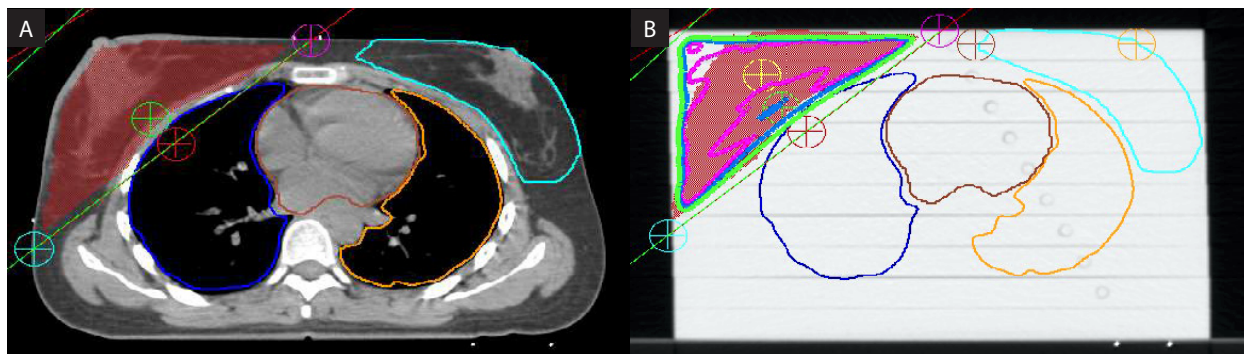


Figure 1. Representative axial CT image of a right breast cancer patient; **A.** Medial marker (purple), lateral marker (light blue), isocenter (red), and breast point (green): 2 cm from isocenter perpendicular to the posterior edge of the tangent beams; **B.** markers for the center of the phantom surface (purple), planning target volume (PTV) point (yellow), the most medial contralateral breast (CLB) point (brown), and CLB below the nipple point (orange) for the phantoms

number of segments were automatically determined based on the volume of PTV, in accordance with the guidelines [13].

Direct machine parameter optimization and the auto-planning module of the Pinnacle³ TPS were used for calculations. The auto-planning settings were not changed in this study. The target optimization goal was 5000 cGy for PTV. Priorities of the OAR were all set to “medium” with compromise in the following optimization presets: ipsilateral lung (ILL) $V_{20} < 15\%$, where V_{20} was defined as the percentage of the volume receiving at least 2000 cGy; CLB maximum dose (D_{max}) 100 cGy; and heart for left breast cancer D_{max} 4000 cGy. Subsequently, the plans were normalized to result in a mean PTV dose of 5000cGy by proportionally changing the MU of both open and IMRT beams.

Dose measurement (PTV and inner and central quadrants of CLB)

All treatment plans were recalculated on a phantom composed of a stack of ten solid water-equivalent slabs with dimensions of $30 \times 30 \times 2 \text{ cm}^3$ (Fig. 1B). Measurements were performed using a 0.6 cm^3 PTW Farmer-type IC (TN30013, PTW Freiburg GmbH, Germany). The IC was inserted at a depth of 1 cm in the slab, located 1 to 12 cm lateral to the center. The posterior edge of the tangent beams intersected the surface of the midline phantom, with constant jaw positions and gantry angle. The collimator angle was adjusted to 0 or 180 degrees. The beam isocenter was located 7.5 cm lateral to the center of the phantom. The number of MU used in the original treatment plan was used to deliver the dose. The IC for the target volume

was placed in a region of uniform prescribed dose calculated in the PTV. ICs were also placed at the most medial CLB point which is the nearest to the medial CLB tissue and the CLB point below the nipple which is the nearest to nipple of CLB. These positions were replicated using the medial markers of the patients from planning CT (Fig. 1B, Fig. 2). These points represented the highest doses in the inner and center quadrants of CLB, and were monitored by ICs at a depth of 1 cm from the surface. Total treatment session time and actual beam-on time were also monitored. Mean dose (D_{mean}), minimal dose (D_{min}), and D_{max} to the IC volume contoured in the phantom were calculated by the TPS.

Data analysis

The homogeneity index (HI) and conformal index (CI) of the target region were compared between the two techniques [15].

HI is calculated using the following formula:

$$HI = (D_{2\%} - D_{98\%}) / D_{50\%} \quad (1)$$

where $D_{2\%}$, $D_{98\%}$, and $D_{50\%}$ are the minimum doses covering by 2%, 98%, and 50%, respectively, of the PTV volume calculated on the dose-volume histogram. The HI formula shows that lower HI values indicate a more homogeneous target dose. HI = 0 (zero) is the ideal value.

CI is calculated using the following formula:

$$CI = (V_{95\text{PTV}})^2 / (V_{\text{PTV}} \times V_{95\%}) \quad (2)$$

where $V_{95\text{PTV}}$ is the PTV volume covered by 95% of the prescription dose, $V_{95\%}$ is the body volume

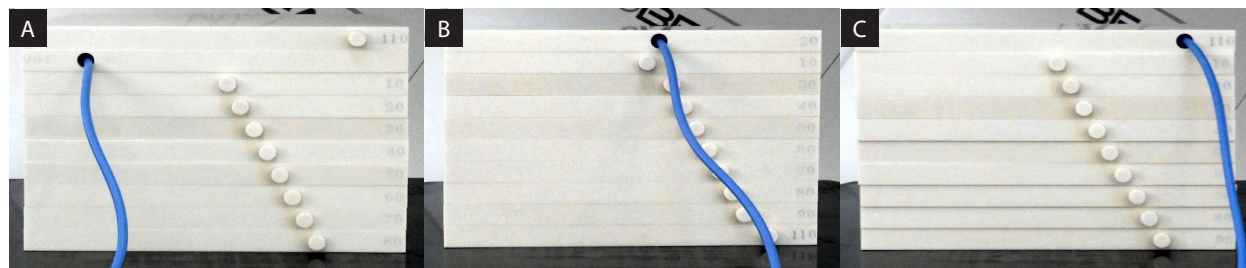


Figure 2. Measurement points in the phantom; **A.** planning target volume (PTV) point; **B.** The most medial contralateral breast (CLB) point; **C.** CLB below the nipple point

receiving 95% of the prescription dose, and V_{ptv} is the target volume. CI takes into account radiation delivery to the target volume and normal tissues. $CI = 1$ is the ideal value.

For OAR, the values of D_{max} and D_{mean} for CLB, and D_{max} and V_{20} for ILL were evaluated and compared in all patients. D_{max} and V_{30} for the heart were investigated in left breast cancer patients.

We defined the plans as acceptable from a clinical perspective when $D_{2\%}$ was below 5350 cGy and $D_{98\%}$ was above 4500 cGy.

Analysis was performed to compare FF and FFF modes. Quantitative data of 20 patients were expressed as mean \pm standard deviation. The results were compared for the two sets of plans with the paired Student's *t*-test. Factors with *p*-values < 0.05 were considered significant. All analyses were performed with SPSS version 25.0 (IBM, Armonk, NY, USA).

Results

Patient dose-volume histograms

The PTV and breast separation between the tangent entry points ranged from 105.2 to 1005.9 cm³ (485.3 ± 287) and 14.1 to 20.8 cm (17.9 ± 2), respectively.

The mean dose-volume histograms used to evaluate the different dose distributions for the FF and FFF techniques are shown in Figure 3. All plans were clinically acceptable as $D_{2\%}$ ranged from 5090 to 5241 cGy for FF and from 5147 to 5321 cGy for FFF. $D_{98\%}$ ranged from 4664 to 4829 cGy for FF and 4512 to 4759 cGy for FFF. HI, CI, and PTV ($D_{98\%}$, $D_{2\%}$, D_{max} , D_{min}) of the target regions in the FF and FFF plans are shown in Table 1. The two types of IMRT plans showed no significant difference in CI of the target region. Although the average dose dif-

ferences of $D_{98\%}$ and $D_{2\%}$ were clinically small (159.9 cGy, 59.9 cGy, respectively), significant differences in HI and PTV doses ($D_{98\%}$, $D_{2\%}$, D_{max} , D_{min}) resulted in worse dose homogeneity within the target volume for FFF ($p < 0.001$).

Dosimetry of OAR within the field and out of the field are presented in Table 1. For the ILL of all 20 patients, D_{max} was significantly higher ($p < 0.001$) but there was a tendency for V_{20} to be lower ($p = 0.051$) in FFF planning. No significant differences were found in the D_{max} and V_{30} to the heart of the ten left breast cancer patients. FF planning showed significantly lower D_{max} and D_{mean} of CLB compared with FFF planning ($p < 0.001$).

IC dose calculation

For PTV points in the phantom, D_{min} calculated across the IC was 5.5% lower in one case; however, others were within 5% of the mean IC doses. All D_{max} values calculated across the IC were within 3% of the mean IC doses. For the most medial CLB point and the CLB below the nipple point, D_{max} and D_{min} calculated across the IC were not within the 5% difference of the mean IC dose. The calculated average dose of the most medial CLB point and the CLB point below the nipple by the TPS were significantly higher in the FFF mode than in the FF mode (8.5 ± 2.5 cGy vs. 7 ± 2.1 cGy, $p < 0.001$ and 2.2 ± 0.6 cGy vs. 1.6 ± 0.5 cGy, $p < 0.001$, respectively).

IC dose measurement

Measured parameters comparing t-IMRT in the FF and FFF modes are listed in Table 2. Delivery time and treatment time were lower for FFF, but the mean time reductions were only 6.1 and 7.6 seconds, respectively. The measured dose of the most medial CLB point and the CLB point

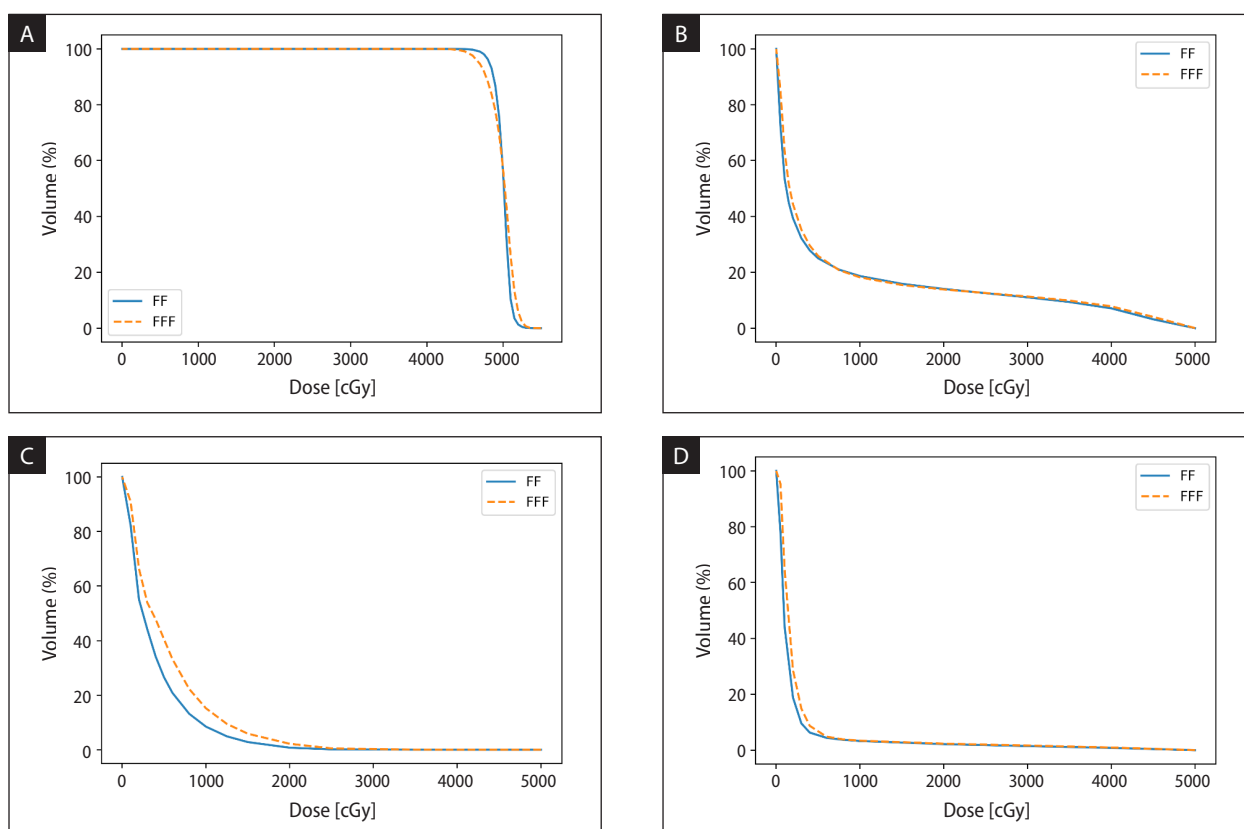


Figure 3. Mean dose-volume histograms for the planning target volume (PTV) (A); ipsilateral lung (ILL) (B), and contralateral breast (CLB) (C) for all patients and heart for left breast cancer patients (D)

Table 1. Comparison of calculated parameters (mean \pm standard deviation) between two tangential intensity modulated radiotherapy (IMRT) plans

Parameter	Flattening-filter	Flattening-filter-free	Difference*	p-value
HI	0.1 \pm 0.01	0.1 \pm 0.02	-0.04 \pm 0.02 (-52.8)	< 0.001
CI	0.8 \pm 0.1	0.8 \pm 0.1	0 \pm 0.1 (-0.5)	0.841
PTV D _{98%} [cGy]	4761.7 \pm 40	4601.8 \pm 74	159.9 \pm 66.1 (3.4)	< 0.001
PTV D _{2%} [cGy]	5174.2 \pm 39.8	5234.1 \pm 54.2	-59.9 \pm 34.4 (-1.2)	< 0.001
PTV D _{max} [cGy]	5337.5 \pm 93.3	5385.9 \pm 115.1	-48.4 \pm 93.1 (-0.9)	0.031
PTV D _{min} [cGy]	4320.1 \pm 145.5	4184 \pm 138.3	136.2 \pm 107.7 (3.2)	< 0.001
ILL D _{max} [cGy]	4917.5 \pm 143	5001.1 \pm 138	-83.7 \pm 63.1 (-1.7)	< 0.001
ILL V ₂₀ (%)	14.1 \pm 5.3	13.9 \pm 5.5	0.2 \pm 0.4 (1.3)	0.051
Heart D _{max} [cGy] [†]	4402.3 \pm 1031.3	4455.2 \pm 1074.6	-52.9 \pm 105.9 (-1.2)	0.149
Heart V ₃₀ (%) [†]	1.9 \pm 2.3	1.7 \pm 1.6	0.2 \pm 1.4 (-11.7)	0.631
CLB D _{max} [cGy]	278.6 \pm 219	320.3 \pm 266.1	-41.7 \pm 55.8 (-15)	0.003
CLB D _{mean} [cGy]	41.4 \pm 13.7	55.4 \pm 17.4	-14 \pm 4 (-33.8)	< 0.001

*Difference between with filter and without filter; † ten left breast cancer patients; HI — homogeneity index; CI — conformal index; PTV — planning target volume; ILL — ipsilateral lung; CLB — contralateral breast

below the nipple were significantly lower in the FFF mode than in FF mode (5.7 ± 1.2 cGy vs. 7.2 ± 1.6 cGy, $p < 0.001$ and 2.3 ± 0.3 vs. 2.9 ± 0.3 , $p < 0.001$, respectively). FFF showed lower per-

centages of out-of-field dose than FF in both the most medial CLB point and the CLB point below the nipple (range, 14.8–26.3% vs. 11.2–22.8%, respectively).

Table 2. Comparison of phantom measured parameters (mean \pm standard deviation) between two tangential intensity modulated radiotherapy (IMRT) plans

Parameter	Flattening-filter	Flattening-filter-free	Difference* (%)	p-value
Monitor Units	268.4 \pm 11	342.5 \pm 21.7	-74.1 \pm 18.4 (-27.6)	< 0.001
Delivery time (second)	49.8 \pm 5.5	43.7 \pm 7.4	6.1 \pm 7.1 (12.2)	0.001
Treatment time (second)	138.8 \pm 12.8	131.2 \pm 10.1	7.6 \pm 11 (5.5)	0.006
Measured dose				
PTV [cGy]	208.7 \pm 5.9	212.8 \pm 7.3	-4.1 \pm 2.4 (-2)	< 0.001
Medial CLB [cGy]	7.2 \pm 1.6	5.7 \pm 1.2	1.5 \pm 0.4 (21.1)	< 0.001
CLB below nipple [cGy]	2.9 \pm 0.3	2.3 \pm 0.3	0.6 \pm 0.1 (20)	< 0.001
Out of dose ratio				
Medial CLB/PTV (%)	3.4 \pm 0.7	2.7 \pm 0.5	0.8 \pm 0.2 (22.6)	< 0.001
CLB below nipple/PTV (%)	1.4 \pm 0.1	1.1 \pm 0.1	0.3 \pm 0.1 (21.5)	< 0.001

*Difference between with filter and without filter; PTV — planning target volume; CLB — contralateral breast; Medial CLB/PTV — dose ratios in points of medial CLB to PTV; CLB below nipple/PTV — dose ratios in points below nipple of CLB to PTV

Discussion

As second breast cancer represents almost a half of all second cancers reported in women with a diagnosis of breast cancer [16], we focused on the assessment of the delivered low radiation dose to the CLB for young women. Many WBI studies have compared fixed-field IMRT plans and volumetric modulated arc therapy (VMAT) plans by irradiated dose distribution of the target region, irradiated dose in nearby normal tissues, or irradiated doses to the CLB [8, 17, 18]. Most of these studies compared plans using the excess absolute risk (EAR), which is a mathematical formula for assessing the risk of a second breast malignancy [19]. EAR is calculated from the organ equivalent dose based on commercial TPS data of the entire CLB dose-volume histogram. Most TPS consider changes in lateral electron transport but do not adequately account for head scatter, which typically contributes more than 40% of the mean out-of-field dose [9]. Comparative planning studies of different treatment techniques using these commercial TPS may not be valid for the assessment of out-of-field low doses to the CLB.

Monte Carlo (MC) simulation is recommended for out-of-field doses when testing new radiotherapy techniques [11]. The MC model is significantly more accurate than other TPS as collimator scatter, leakage through the collimators (including interleaf leakage), and electron contamination are modeled [9]. We used ten solid water equivalent slabs, which is a common methodology for dose measurement.

This enabled us to measure points related to the inner and central quadrants of the CLB where higher incidences of CLB cancer have been noted [3]. FF planning showed significantly lower D_{max} and D_{mean} of the CLB in patient dose-volume histograms than FFF planning. Although the most medial CLB point and the CLB below the nipple point were not in the region of uniform dose within the field, and calculations were thus inaccurate, we also found a lower calculated dose of the most medial CLB point and the CLB point below the nipple for FF by the TPS. In contrast, by dose measurement, the FFF mode delivered significantly lower out-of-field dose in both the most medial CLB point and the CLB point below the nipple than FF. This was caused by inadequate consideration of head scatter by the TPS.

Pignol et al. [12] reported that t-IMRT and the virtual wedge technique yielded smaller doses than physical wedge compensation to neighboring solid organs, including the CLB for WBI. They used MC simulation with a realistic anthropomorphic phantom based on patient anatomy. Several articles have reported lower CLB doses with t-IMRT or with a field-in-field technique than with multibeam IMRT and partial-arcs VMAT for WBI [8, 17, 18, 20]. We selected t-IMRT in this study as, when secondary cancer risk is a major concern, t-IMRT is the preferred treatment option for WBI.

An FF beam profile is not required for varying radiation intensity of each beam because of the superposition of multiple intensity patterns for IMRT. Reduced treatment head leakage by the use of FFF beams leading to reduced peripheral dose has been

reported [4-6]. Kragl et al. [5] used a Farmer-type IC placed in a solid water slab phantom to assess IMRT treatment plans. They compared FF and FFF beams, and found average reductions of peripheral dose in FFF of 16% for the prostate at 18 cm distant from the field edge and of 18% for the head and neck at 20 cm distant from the field edge. Our measured dose of the most medial CLB point and the CLB point below the nipple were significantly lower in the FFF mode than in the FF mode, with mean reductions of 21.1% and 20%, respectively, and were similar to Kragl et al.'s results [5].

Auto-planning algorithms offer “one click planning” by automatically generating additional structures, optimization of parameter setup, and final inverse optimization. The auto-planning technique was compared with manual planning for WBI using t-IMRT, and it was found that auto-planning improved planning efficiency and plan quality [21]. In our study, we excluded planner dependence by using auto-planning.

Since the American Society for Radiation Oncology recommended against the routine use of IMRT (*vs.* three-dimensional conformal radiotherapy) in breast cancer patients in 2013, the use of IMRT has decreased in hospital-based clinics [22]. There is no obvious evidence that using IMRT and VMAT decreases CLB cancer risk compared with t-IMRT or field-in-field three-dimensional conformal radiotherapy. We found that t-IMRT using FFF decreased low-dose irradiation to the CLB, as measured by solid water-equivalent slab phantoms. Using this method, several different treatment plans that resemble clinical situations are available to analyze in hospital-based clinics with low cost. This method can also be used to assess new radiotherapy techniques for WBI.

Limitations

Our study had some limitations. First, we used water-equivalent phantoms, which did not consider tissue heterogeneities such as the lungs. Second, we chose solid water-equivalent slab phantoms; these were similar in size to the patients, but unlike anthropomorphic phantoms, the shapes were not based on realistic patient anatomy. Third, we could not use the model for assessing EAR, as we could not acquire the accurate organ equivalent dose of the entire CLB. Finally, we evaluated only the CLB and not other out-of-field OARs.

Conclusions

We compared the FF and FFF modes of automated tangential IMRT planning for young breast cancer patients. All plans were clinically acceptable. There was less dose homogeneity within the target volume for the FFF mode, but there was no difference in conformity between the two IMRT plans. In contrast to the calculation results by the TPS, FFF reduced the measured out-of-field dose of the most medial CLB point and the CLB point below the nipple. Using our method, several different WBI plans that resemble clinical situations are available to analyze the selected CLB points without MC simulation.

Conflicts of interest

The Radiotherapy Department of Yokohama City Medical Center has research cooperation with Nihon Denshi Ohyo, Ltd. Authors declare that they have no competing interests.

Funding

Ichiro Ogino report grants; Japan Society for the Promotion of Science Grants-in-Aid for Scientific Research 17K10487.

References

1. Boice JD, Harvey EB, Blettner M, et al. Cancer in the contralateral breast after radiotherapy for breast cancer. *N Engl J Med.* 1992; 326(12): 781–785, doi: [10.1056/NEJM199203193261201](https://doi.org/10.1056/NEJM199203193261201), indexed in Pubmed: [1538720](https://pubmed.ncbi.nlm.nih.gov/1538720/).
2. Gao X, Fisher SG, Emami B. Risk of second primary cancer in the contralateral breast in women treated for early-stage breast cancer: a population-based study. *Int J Radiat Oncol Biol Phys.* 2003; 56(4): 1038–1045, doi: [10.1016/s0360-3016\(03\)00203-7](https://doi.org/10.1016/s0360-3016(03)00203-7), indexed in Pubmed: [12829139](https://pubmed.ncbi.nlm.nih.gov/12829139/).
3. Stovall M, Smith SA, Langholz BM, et al. Women's Environmental, Cancer, and Radiation Epidemiology Study Collaborative Group. Dose to the contralateral breast from radiotherapy and risk of second primary breast cancer in the WECARE study. *Int J Radiat Oncol Biol Phys.* 2008; 72(4): 1021–1030, doi: [10.1016/j.ijrobp.2008.02.040](https://doi.org/10.1016/j.ijrobp.2008.02.040), indexed in Pubmed: [18556141](https://pubmed.ncbi.nlm.nih.gov/18556141/).
4. Wijesooriya K. Part I: Out-of-field dose mapping for 6X and 6X-flattening-filter-free beams on the TrueBeam for extended distances. *Med Phys.* 2019; 46(2): 868–876, doi: [10.1002/mp.13362](https://doi.org/10.1002/mp.13362), indexed in Pubmed: [30589941](https://pubmed.ncbi.nlm.nih.gov/30589941/).
5. Kragl G, Baier F, Lutz S, et al. Flattening filter free beams in SBRT and IMRT: dosimetric assessment of peripheral doses. *Z Med Phys.* 2011; 21(2): 91–101, doi: [10.1016/j.zemedi.2010.07.003](https://doi.org/10.1016/j.zemedi.2010.07.003), indexed in Pubmed: [20888199](https://pubmed.ncbi.nlm.nih.gov/20888199/).
6. Dobler B, Maier J, Knott B, et al. Second Cancer Risk after simultaneous integrated boost radiation therapy of right sided breast cancer with and without flattening filter.

- Strahlenther Onkol. 2016; 192(10): 687–695, doi: [10.1007/s00066-016-1025-5](https://doi.org/10.1007/s00066-016-1025-5), indexed in Pubmed: [27534409](https://pubmed.ncbi.nlm.nih.gov/27534409/).
7. Karpf D, Sakka M, Metzger M, et al. Left breast irradiation with tangential intensity modulated radiotherapy (t-IMRT) versus tangential volumetric modulated arc therapy (t-VMAT): trade-offs between secondary cancer induction risk and optimal target coverage. *Radiat Oncol.* 2019; 14(1): 156, doi: [10.1186/s13014-019-1363-4](https://doi.org/10.1186/s13014-019-1363-4), indexed in Pubmed: [31477165](https://pubmed.ncbi.nlm.nih.gov/31477165/).
 8. Zhang HW, Hu Bo, Xie C, et al. Dosimetric comparison of three intensity-modulated radiation therapies for left breast cancer after breast-conserving surgery. *J Appl Clin Med Phys.* 2018; 19(3): 79–86, doi: [10.1002/acm2.12287](https://doi.org/10.1002/acm2.12287), indexed in Pubmed: [29524290](https://pubmed.ncbi.nlm.nih.gov/29524290/).
 9. Joosten A, Matzinger O, Jeanneret-Sozzi W, et al. Evaluation of organ-specific peripheral doses after 2-dimensional, 3-dimensional and hybrid intensity modulated radiation therapy for breast cancer based on Monte Carlo and convolution/superposition algorithms: implications for secondary cancer risk assessment. *Radiother Oncol.* 2013; 106(1): 33–41, doi: [10.1016/j.radonc.2012.11.012](https://doi.org/10.1016/j.radonc.2012.11.012), indexed in Pubmed: [23351844](https://pubmed.ncbi.nlm.nih.gov/23351844/).
 10. Aziz MH, Schneider F, Clausen S, et al. Can the risk of secondary cancer induction after breast conserving therapy be reduced using intraoperative radiotherapy (IORT) with low-energy x-rays? *Radiat Oncol.* 2011; 6: 174, doi: [10.1186/1748-717X-6-174](https://doi.org/10.1186/1748-717X-6-174), indexed in Pubmed: [22176703](https://pubmed.ncbi.nlm.nih.gov/22176703/).
 11. Donovan EM, James H, Bonora M, et al. Second cancer incidence risk estimates using BEIR VII models for standard and complex external beam radiotherapy for early breast cancer. *Med Phys.* 2012; 39(10): 5814–5824, doi: [10.1118/1.4748332](https://doi.org/10.1118/1.4748332), indexed in Pubmed: [23039620](https://pubmed.ncbi.nlm.nih.gov/23039620/).
 12. Pignol JP, Keller BM, Ravi A. Doses to internal organs for various breast radiation techniques—implications on the risk of secondary cancers and cardiomyopathy. *Radiat Oncol.* 2011; 6: 5, doi: [10.1186/1748-717X-6-5](https://doi.org/10.1186/1748-717X-6-5), indexed in Pubmed: [21235766](https://pubmed.ncbi.nlm.nih.gov/21235766/).
 13. Purdie TG, Dinniwell RE, Letourneau D, et al. Automated planning of tangential breast intensity-modulated radiotherapy using heuristic optimization. *Int J Radiat Oncol Biol Phys.* 2011; 81(2): 575–583, doi: [10.1016/j.ijrobp.2010.11.016](https://doi.org/10.1016/j.ijrobp.2010.11.016), indexed in Pubmed: [21237584](https://pubmed.ncbi.nlm.nih.gov/21237584/).
 14. Radiation Therapy Oncology Group: Breast cancer atlas for radiation therapy planning: Consensus definitions. <https://www.nrgoncology.org/ciro-breast> (July 18 2021).
 15. Kusters JM, Bzdusek K, Kumar P, et al. Automated IMRT planning in Pinnacle : A study in head-and-neck cancer. *Strahlenther Onkol.* 2017; 193(12): 1031–1038, doi: [10.1007/s00066-017-1187-9](https://doi.org/10.1007/s00066-017-1187-9), indexed in Pubmed: [28770294](https://pubmed.ncbi.nlm.nih.gov/28770294/).
 16. Taylor C, Correa C, Duane FK, et al. Early Breast Cancer Trialists' Collaborative Group. Estimating the Risks of Breast Cancer Radiotherapy: Evidence From Modern Radiation Doses to the Lungs and Heart and From Previous Randomized Trials. *J Clin Oncol.* 2017; 35(15): 1641–1649, doi: [10.1200/JCO.2016.72.0722](https://doi.org/10.1200/JCO.2016.72.0722), indexed in Pubmed: [28319436](https://pubmed.ncbi.nlm.nih.gov/28319436/).
 17. Fogliata A, De Rose F, Franceschini D, et al. Critical Appraisal of the Risk of Secondary Cancer Induction From Breast Radiation Therapy With Volumetric Modulated Arc Therapy Relative to 3D Conformal Therapy. *Int J Radiat Oncol Biol Phys.* 2018; 100(3): 785–793, doi: [10.1016/j.ijrobp.2017.10.040](https://doi.org/10.1016/j.ijrobp.2017.10.040), indexed in Pubmed: [29249528](https://pubmed.ncbi.nlm.nih.gov/29249528/).
 18. Hacıslamoglu E, Cinar Y, Gurcan F, et al. Secondary cancer risk after whole-breast radiation therapy: field-in-field versus intensity modulated radiation therapy versus volumetric modulated arc therapy. *Br J Radiol.* 2019; 92(1102): 20190317, doi: [10.1259/bjr.20190317](https://doi.org/10.1259/bjr.20190317), indexed in Pubmed: [31295011](https://pubmed.ncbi.nlm.nih.gov/31295011/).
 19. Schneider U, Sumila M, Robotka J, et al. Dose-response relationship for breast cancer induction at radiotherapy dose. *Radiat Oncol.* 2011; 6: 67, doi: [10.1186/1748-717X-6-67](https://doi.org/10.1186/1748-717X-6-67), indexed in Pubmed: [21651799](https://pubmed.ncbi.nlm.nih.gov/21651799/).
 20. Abo-Madyan Y, Aziz MH, Aly MM, et al. Second cancer risk after 3D-CRT, IMRT and VMAT for breast cancer. *Radiother Oncol.* 2014; 110(3): 471–476, doi: [10.1016/j.radonc.2013.12.002](https://doi.org/10.1016/j.radonc.2013.12.002), indexed in Pubmed: [24444525](https://pubmed.ncbi.nlm.nih.gov/24444525/).
 21. Guo B, Shah C, Xia P. Automated planning of whole breast irradiation using hybrid IMRT improves efficiency and quality. *J Appl Clin Med Phys.* 2019; 20(12): 87–96, doi: [10.1002/acm2.12767](https://doi.org/10.1002/acm2.12767), indexed in Pubmed: [31743598](https://pubmed.ncbi.nlm.nih.gov/31743598/).
 22. Torres MA, Gogineni K, Howard DH. Intensity-Modulated Radiation Therapy in Breast Cancer Patients Following the Release of a Choosing Wisely Recommendation. *J Natl Cancer Inst.* 2020; 112(3): 314–317, doi: [10.1093/jnci/djz198](https://doi.org/10.1093/jnci/djz198), indexed in Pubmed: [31647560](https://pubmed.ncbi.nlm.nih.gov/31647560/).